ELSEVIER

Carbohydrate Research 278 (1995) 27–41

CARBOHYDRATE RESEARCH

# Hydration of α-maltose and amylose: molecular modelling and thermodynamics study

Christophe Fringant [a], Igor Tvaroska [b,*], Karim Mazeau [a], Marguerite Rinaudo [a], Jacques Desbrieres [a]

[a] *Centre de Recherches sur les Macromolécules Végétales, CNRS, B.P. 53, F-38041 Grenoble, France*
[b] *Institute of Chemistry, Slovak Academy of Sciences, SK-84238 Bratislava, Slovak Republic*

Received 31 March 1995; accepted in revised form 15 June 1995

**Abstract**

Hydration of α-maltose and amylose were investigated using molecular modelling and thermodynamics methods. The structure and energy of hydration of three low-energy conformers of α-maltose were determined by the MM3 molecular mechanics method. The hydration structure was found to be sensitive to the conformation of α-maltose and hydration numbers 10 or 11 were estimated for the different conformers. Differential scanning calorimetry and thermogravimetric analysis were used to determine the number of water molecules specifically bonded (non-freezing water) to amylose and different samples of α-maltose. Due to high crystallinity of α-maltose samples, the observed non-freezing water content was lower than predicted by molecular modelling. In contrast, the experimental number of non-freezing molecules of water per D-glucopyranose residue for amorphous amylose ($n_h = 3.8$) is in good accordance with the value of 3.8 extracted from our calculations.

*Keywords:* Maltose; Amylose; Molecular modelling; Differential scanning calorimetry; Hydration; Non-freezing water; Hydrogen bonding

## 1. Introduction

Water adsorption has a great influence on physical properties of materials and particularly on swelling and softening. As a consequence, solubility, hydrating power (in cosmetics) and mechanical properties will be directly affected. Hydration pattern depends on the number and the nature of sites able to adsorb water molecules such as

* Corresponding author.


*SSDI* 0008-6215(95)00232-4

hydroxyl or ionic groups but also on the crystallinity of materials. Results on cellulose-based materials showed [1–3] that water fixation does not occur within crystalline zones where intermolecular hydrogen bonds are very strong. Only the surfaces of such zones are accessible [4,5]. The introduction of water molecules within amorphous zones increases the mobility of macromolecular chains and hence modifies thermodynamic properties such as glass transition and swelling. This water sorption is particularly important when studying polysaccharide-based materials. For many years, a lot of research has been devoted to the use of an easily renewable polymer in new materials: starch. A main problem encountered until now is water sensitivity of such materials [6]. Therefore, we have undertaken a research program dealing with chemical modification of starch in order to reinforce its hydrophobicity [7]. In this respect, the understanding of molecular interactions between water and amorphous polysaccharide is of crucial importance. Recently, the hydration pattern of amylose in crystal structures has been investigated [8]. However, such studies cannot explain the water sensitivity of starch-based materials as starch is destructured and only very partly crystalline in these materials. In order to offer a new insight into water sorption, we have examined in this study the structure and energy of hydration sites of α-maltose by molecular modelling and the hydration of α-maltose and amorphous amylose using differential scanning calorimetry and thermogravimetric analysis.

Recently, molecular dynamics simulation of β-maltose in two different conformations in vacuum and in aqueous solution has been used to examine the types of hydrogen bonds made by maltose [9]. However, little is known about the specific interaction of water molecules and the amorphous maltose at the molecular level. The crystal structure of β-maltose has been determined to high resolution by neutron diffraction [10]. The crystal conformation has been found to be stabilised by an intramolecular hydrogen bond between the O-2′ hydroxyl group of the non-reducing residue and the O-3 hydroxyl group of the reducing residue. The O-2′ · · · O-3 hydrogen bond was also observed in the crystal structures of α-maltose [11] and methyl β-maltoside [12]. Maltose has long been the subject of molecular mechanics studies and recently, relaxed conformational energy maps have been calculated using several different force fields [13–15]. The relaxed conformational energy studies have generally demonstrated that maltose has several low energy conformations in vacuum, some of which possess the intramolecular O-2′ · · · O-3 hydrogen bond, but with at least one important low-energy structure, which for geometric reasons, cannot form this hydrogen bond. Both the experimental studies [16,17] and the calculations using the continuum model of solvation [18] imply that, in the solution, there is a shift away from the crystal structure conformation.

## 2. Experimental

*Materials.*—The sample of crystalline α-maltose [α-D-glucopyranosyl-(1 → 4)-α-D-glucopyranose] monohydrate was obtained from Sigma Chemical Co., and was used in this study as received without further purification. Some special preparations of maltose samples were made in order to decrease the crystallinity. They consisted of dissolving

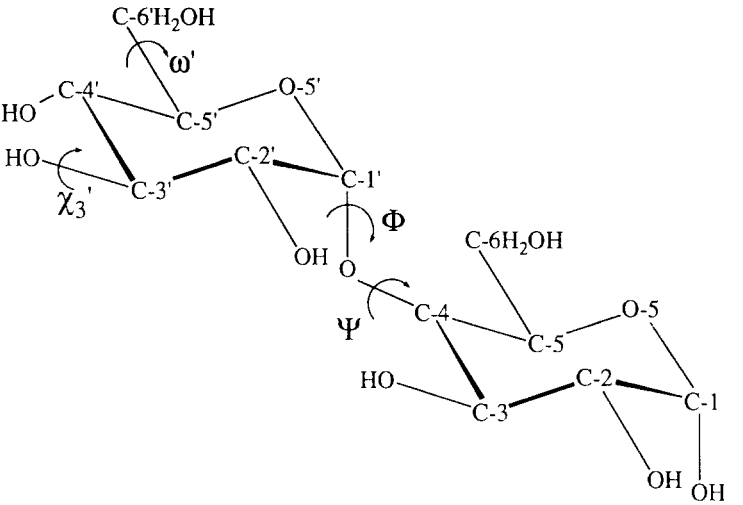


Scheme 1.

commercial maltose in pure water at different concentrations and freeze drying of the solution. Another preparation was to evaporate a concentrated solution to dryness and to dry the resulting glassy product under vacuum at 50°C for several days. All these preparations did not allow us to obtain completely amorphous maltose as revealed by X-ray diffraction measurements. Amylose [(1 → 4)-α-D-glucopyranan] sample was obtained from Avebe Co. (Veendam, Holland), and was used as received. The crystallinity was approximately 15%.

*Nomenclature.*—The recommendations and symbols proposed by the IUPAC-IUB Commission [19] were used. A schematic representation of the disaccharides and the numbering of atoms is shown in Scheme 1. The relative orientation of the monosaccharide residues about the glycosidic linkage is based on the values of two torsion angles $\Phi$(O-5′–C-1′–O-1′–C-4) and $\Psi$(C-1′–O-1′–C-4–C-3). The orientation of the hydroxymethyl groups is defined by the torsion angles $\omega$(C-4–C-5–C-6–O-6) and $\omega'$(C-4′–C-5′–C-6′–O-6′). The orientation of hydroxyl hydrogen atoms is defined as $\chi_i$ = C-$i$ − 1–C-i–O-i–H(O-$i$) where $i$ = 2′, 3′, 4′, 6′, 1, 2, 3 and 6. Depending on the type of hydrogen bonding considered [$O_w \cdots$ H(O-$i$)–O-$i$ or $O_w$–$H_w \cdots$ O-$i$], the $r$ and $\Theta$ parameters were defined as it follows. For the $O_w$–$H_w \cdots$ O-$i$ interaction, $r$ is defined as the distance between the atoms O-$i$ and $H_w$ atoms and $\Theta$ is the C-$i$–O-$i$–$H_w$–$O_w$ dihedral angle. In the case of the $O_w \cdots$ H(O-$i$)–O-$i$ interaction, the oxygen atom $O_w$ has been placed in the direction of the O-$i$–H(O-$i$) bond of the interacting hydroxyl group. Here, $r$ represents the distance between the H(O-$i$) and $O_w$ atoms, and dihedral angle $\Theta$ represents the orientation of hydroxyl hydrogen atoms defined by torsion angle $\chi_i$.

*Molecular modelling.*—The starting geometry of the disaccharide was derived from the monomer library of the QUANTA software (Molecular Simulation, Burlington, MA). ($\Phi$,$\Psi$) Relaxed maps were computed by rotating the residues around the

glycosidic linkage on a 10° grid. At each point of the grid, geometry optimisation was performed using the MM3 molecular mechanics program [20,21] with a dielectric constant $\epsilon = 1.5$. To minimise the energy, the Cartesian coordinates of each atom except those defining the $\Phi$ and $\Psi$ torsion angles were allowed to vary. The final location of minima were found for each local low-energy region of the $(\Phi,\Psi)$ map by non-restricted minimisation.

The first hydration shell of three lowest-energy conformers of $\alpha$-maltose was calculated in two steps. In the first one, the minima on energy surfaces describing the interaction between water molecule and one of the maltose hydroxyl groups or oxygen atoms were found and their structure was determined. In the next step, the $\alpha$-maltose–$n$ water complex was investigated. For this purpose, one water molecule was placed at each of the previously determined hydration sites. The structure of the complex was then optimised allowing only the atoms of the water molecules to move. As our interest is mainly focused on the first hydration shell, the water molecules that were not linked directly to $\alpha$-maltose were discarded for the next step of the calculation. In the final step of calculation, the structure of hydrated maltose was optimised without constraints with the exceptions of atoms defining the $\Phi$ and $\Psi$ dihedral angles.

*Differential scanning calorimetry (DSC).*—A Perkin–Elmer differential scanning calorimeter (DSC7), equipped with a cooling device, was used to determine the amount of freezing water. DSC curves were obtained in the temperature range of −60°C to 25°C. Indium ($T_m$ = 156.64°C) and *n*-dodecane ($T_m$ = −9.65°C) were used for calibration. DSC curves were obtained upon heating with a scanning rate of 2°C/min. The cooling speed was 200°C/min and 10 min were allowed for equilibration at the starting temperature. Sample enthalpies were calculated using pure water as reference. Sample weights varied between 5 and 15 mg. The samples were weighted in aluminium capsules, which were then sealed. During preparation, samples were exposed to ambient atmosphere for approximately 1 min.

*Thermogravimetric analysis (TGA).*—A Setaram thermogravimetric analyzer 92-12 was used to determine the total water content of the samples. Hydrated sample weight varied around 30 mg. Scanning rate and temperature interval were respectively 5°C/min and 20–130°C. Tests were maintained until the derivative of the weight loss curve equalled zero. During loading, samples were exposed to ambient atmosphere for an average period of 1 min.

*Relative humidity (RH).*—The different moisture levels used were obtained by exposing the powders to the vapour of different saturated solutions in closed desiccators: $LiCl \cdot H_2O$ for 15%, $CaCl_2 \cdot 6H_2O$ for 32%, $K_2CO_3 \cdot 2H_2O$ for 44%, $Ca(NO_3)_2 \cdot 4H_2O$ for 56%, NaCl for 76%, $K_2CrO_4$ for 88% and $CuSO_4 \cdot 5H_2O$ for 98%. Samples were conditioned in desiccators for a period of 3 weeks to ensure equilibrium.

## 3. Results and discussion

*The relaxed conformational energy map for α-maltose.*—The MM3 potential energy map for $\alpha$-maltose is shown in Fig. 1. The energy is plotted as a function of the glycosidic torsion angles $\Phi$ and $\Psi$. The map is similar to the MM3 map already

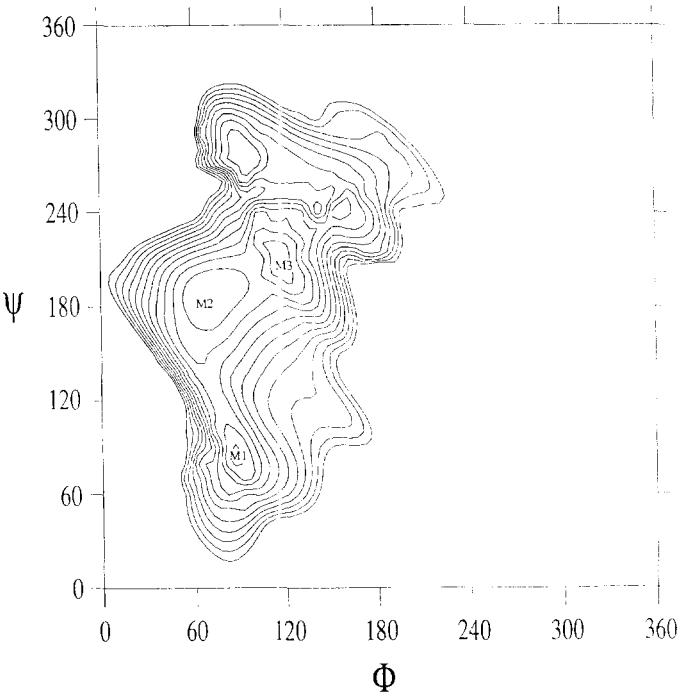


Fig. 1. MM3-generated relaxed-residue potential energy map for α-maltose. Contours are drawn in 1 kcal/mol above the lowest energy conformer. Abbreviations designate the minima referred to in the text and in tables.

reported [15]. Minor differences between both maps can be attributed to the use of different values of dielectric constant. Two low-energy regions appear on the map. The dominant region contains the lowest two of the three minima found on the maps. One minimum M2 appears at $(\Phi, \Psi) = (64°, 189°)$, the second minimum M3 at $(\Phi, \Psi) = (105°, 211°)$ and the third minimum M1 is found in the second low energy region at $(\Phi, \Psi) = (78°, 87°)$. All three minima are within 1.50 kcal/mol. All three final minima were used to investigate the hydration sites of α-maltose.

*Geometry and energetics of maltose–water complexes.*—Each of the 11 oxygens of α-maltose can act as a donor and each of the eight hydroxyl groups as an acceptor of hydrogen bond with water molecules. Prerequisite for building and understanding the hydration structure of maltose is a detailed description of the structure of the complexes between water and individual hydroxyl groups. A thorough search of energy surfaces gave 18 different minima for interaction between α-maltose and the water molecule. The calculated structures agree reasonably well with ab initio calculations on alcohol–water complexes [22,23]. As an exhaustive presentation of the results obtained is outside the scope of this paper, we present here only a survey of the water stereochemistry in these minima which is schematically illustrated in Fig. 2.

The analysis of the final structures revealed that possible hydrogen bond arrangements between water and α-maltose can be divided into six groups. As can be seen from

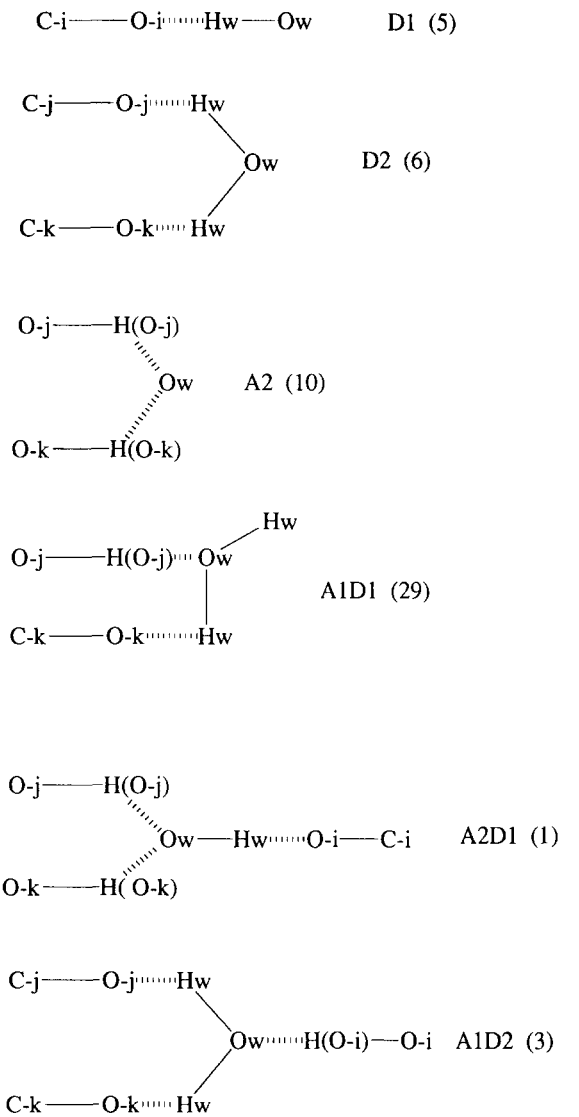


Fig. 2. Schematic depiction of six possible hydrogen bond arrangements in complexes between α-maltose and water molecule. Abbreviations designate the type and numbers represent occurrence in 54 complexes.

Fig. 2, the majority of water molecules in 54 complexes display one acceptor–one donor (A1D1) or two acceptors (A2) patterns. These two arrangements account for more than 70% of all the possible hydrogen-bond structures. It is noteworthy that, in MD simulation of maltose in aqueous solution [9], a large fraction of the first hydration shell water molecules was found in arrangement corresponding to the A2, D2 and A1D1 arrangements. The calculated equilibrium O · · · H distances are in the interval from

1.740 to 1.899 Å and the mean value of O · · · H is 1.793 Å. It appears that, in three complexes, the O · · · H distance is larger than 1.95 Å. A comparison of the O · · · H values clearly indicates that the $O_w$ · · · H distances are shorter than the O · · · $H_w$ distances, as expected from the greater acceptor tendency of water molecules. The mean value for $O_w$ · · · H distances is 1.781 Å whereas the mean value for O · · · $H_w$ distances is 1.805 Å. The O–H · · · O bond angle have a distribution ranging from 120 to 178° with a mean value of 154°.

The crystal structures of carbohydrate hydrates provide useful data for a comparison. However, for stereochemical and packing reasons, this comparison is only qualitative. It has been shown [24–26] that the mean O–H · · · $O_w$ distance in 188 hydrates is 1.83 Å and the mean O–$H_w$ · · · O distance in 82 hydrates is 1.90 Å. These values are in reasonable agreement with our calculated values. The calculated O · · · O distances are in the interval from 2.390 to 2.971 Å and the mean O · · · O distance is 2.641 Å. This value can be compared to the mean O · · · O distance of 2.77 Å found for alcohol and carbohydrates. There has been considerable discussion concerning the direct relationship between hydrogen-bond strength and length. A simple relationship has been obtained for the complexes between water and alcohols [27]. However, our results do not allow to establish such a dependence. The hydrogen bond energy is in the interval from 4 kcal/mol for the D1 arrangement to 13 kcal/mol for the A1D1 arrangement. The mean value of the interaction energy calculated from all minima is 9.35 kcal/mol.

The above positions of water molecules were used to build the first hydration shell for each of three α-maltose conformers. Due to spatial proximity of hydration sites, some water molecules were expelled from their original position during optimisation. Therefore, those water molecules that interacted only with any of the other water molecules were eliminated, leaving only water molecules interacting directly with the α-maltose molecule. Using the geometrical criteria, for the M1 and M3 conformers 11 water molecules are contributing to the first hydration shell, whereas only 10 water molecules were found for the M2 conformer. In this conformer, one of two ring oxygens is not an acceptor of hydrogen bond. The structure of these complexes is shown in Fig. 3 and the main geometrical features are listed in Tables 1–3.

A comparison of the structure of α-maltose conformers in vacuum and in hydrated complexes revealed that hydration imposed several geometrical changes. An increase of internal energy of α-maltose is compensated by an increase in the interaction energy. As can be seen from Tables 1–3 and Fig. 3, most of the hydroxyl groups are involved in two hydrogen bonds, one as an acceptor and one as a donor. As well, most of the water molecules are simultaneously hydrogen bonded to more than one hydroxyl group. A comparison of the stabilisation energy per water molecule revealed that, in all three complexes, a large stabilisation per water molecule is found relative to individual minima. It reaches 10.69 kcal/mol for the M2, 10.95 kcal/mol for the M3, and 11.05 kcal/mol for the M1 conformer. These stabilisation energies are larger than the mean value of water–maltose interaction energy 9.35 kcal. The enhancement from 1.3 to 1.7 kcal/mol per water molecule may be interpreted as a cooperative effect.

*Non-freezing water in α-maltose and amylose.*—Differential scanning calorimetry and thermogravimetric techniques allow the determination of different types of water molecules [28]. Water molecules demonstrating a first order transition will be called

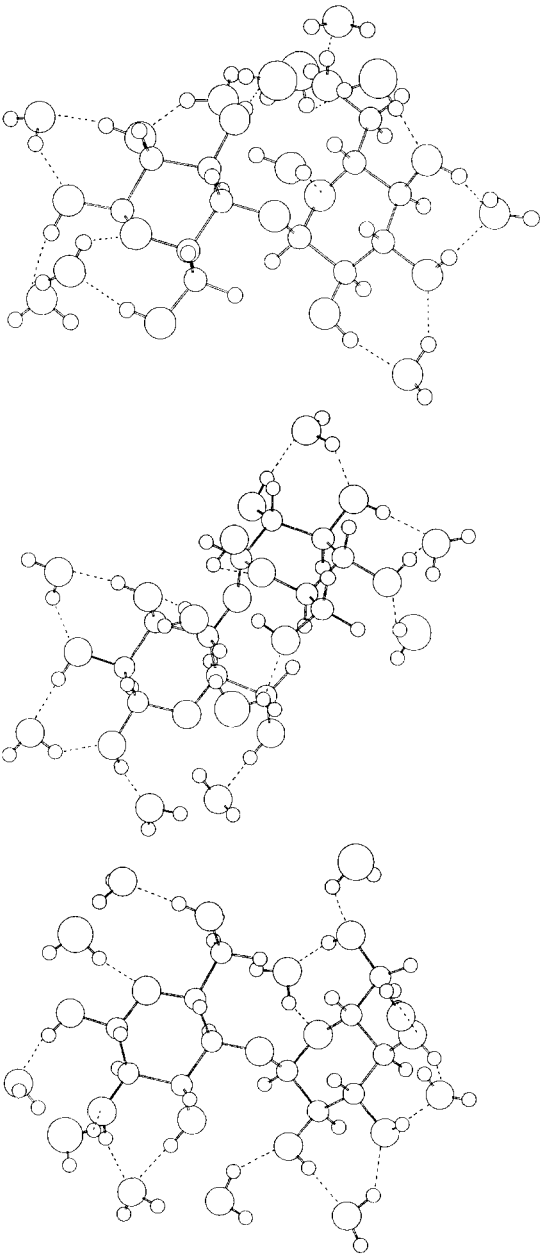

Fig. 3. Molecular representation of the hydration shells of three lowest energy conformers of α-maltose.

''freezing water''; molecules in strong interaction with polymeric sites without such transition are called ''non-freezing water''. Water molecules whose melting point is at 0°C will be called ''free water''. For both products, α-maltose monohydrate and

Table 1
MM3 calculated structural data of hydration shell for M1 conformer of α-maltose [a]

| O-*i* | HB type | *r*(O · · · H) | *r*(O-*i* · · · Ow) | θ*i* | O-*j* | HB type | *r*(O · · · H) | *r*(O-*j* · · · Ow) | θ*j* |
|---|---|---|---|---|---|---|---|---|---|
| O-1 | O-*i* · · · Hw | 1.783 | 2.586 | 140.2 | O-2 | H(O-*j*) · · · Ow | 1.739 | 2.669 | 166.2 |
| O-1 | H(O-*i*) · · · Ow | 1.753 | 2.665 | 160.0 | | | | | |
| O-6 | H(O-*i*) · · · Ow | 1.779 | 2.696 | 161.4 | O-5 | O-*j* · · · Hw | 1.805 | 2.565 | 134.9 |
| O-2 | O-*i* · · · Hw | 1.812 | 2.570 | 134.6 | O-3 | H(O-*j*) · · · Ow | 1.774 | 2.592 | 142.4 |
| O-3 | O-*i* · · · Hw | 1.745 | 2.674 | 165.3 | | | | | |
| O-5′ | O-*i* · · · Hw | 1.819 | 2.753 | 167.5 | | | | | |
| O-6′ | O-*i* · · · Hw | 1.755 | 2.689 | 167.9 | | | | | |
| O-6′ | H(O-*i*) · · · Ow | 1.741 | 2.664 | 163.6 | | | | | |
| O-4′ | H(O-*i*) · · · Ow | 1.774 | 2.617 | 146.3 | O-3′ | H(O-*j*) · · · Ow | 1.753 | 2.668 | 161.1 |
| O-3′ | O-*i* · · · Hw | 1.776 | 2.598 | 143.0 | O-2′ | H(O-*j*) · · · Ow | 1.749 | 2.676 | 164.7 |
| O-4′ | O-*i* · · · Hw | 1.816 | 2.751 | 167.7 | | | | | |

[a] Distances in Å; angles in degrees; energies in kcal/mol.

Table 2
MM3 calculated structural data of hydration shell for M2 conformer of α-maltose [a]

| O-*i* | HB type | *r*(O · · · H) | *r*(O-*i* · · · Ow) | θ*i* | O-*j* | HB type | *r*(O · · · H) | *r*(O-*j* · · · Ow) | θ*j* |
|---|---|---|---|---|---|---|---|---|---|
| O-1 | O-*i* · · · Hw | 1.783 | 2.585 | 140.1 | O-2 | H(O-*j*) · · · Ow | 1.739 | 2.680 | 171.0 |
| O-1 | H(O-*i*) · · · Ow | 1.722 | 2.651 | 165.5 | | | | | |
| O-2 | O-*i* · · · Hw | 1.776 | 2.602 | 143.5 | O-3 | H(O-*j*) · · · Ow | 1.739 | 2.664 | 164.3 |
| O-3 | O-*i* · · · Hw | 1.753 | 2.657 | 158.1 | O-6′ | H(O-*j*) · · · Ow | 1.843 | 2.674 | 144.4 |
| O-6′ | O-*i* · · · Hw | 1.816 | 2.522 | 129.0 | | | | | |
| O-5′ | O-*i* · · · Hw | 1.816 | 2.707 | 155.4 | | | | | |
| O6 | H(O-*i*) · · · Ow | 1.809 | 2.726 | 161.1 | O-5 | O-*j* · · · Hw | 1.813 | 2.543 | 131.2 |
| O-2′ | H(O-*i*) · · · Ow | 1.754 | 2.683 | 165.7 | O-3′ | O-*j* · · · Hw | 1.779 | 2.596 | 142.3 |
| O-3′ | H(O-*i*) · · · Ow | 1.744 | 2.660 | 161.4 | O-4′ | H(O-*j*) · · · Ow | 1.822 | 2.582 | 134.9 |
| O-4′ | O-*i* · · · Hw | 1.817 | 2.592 | 136.8 | | | | | |

[a] Distances in Å; angles in degrees; energies in kcal/mol.

Table 3
MM3 calculated structural data of hydration shell for M3 conformer of α-maltose [a]

| O-*i* | HB type | *r*(O · · · H) | *r*(O-*i* · · · Ow) | θ*i* | O-*j* | HB type | *r*(O · · · H) | *r*(O-*j* · · · Ow) | θ*j* |
|---|---|---|---|---|---|---|---|---|---|
| O-1 | O-*i* · · · Hw | 1.910 | 2.404 | 110.0 | O-5 | O-*j* · · · Hw | 1.817 | 2.701 | 153.5 |
| O-1 | H(O-*i*) · · · Ow | 1.723 | 2.659 | 168.7 | O-2 | O-*j* · · · Hw | 1.891 | 2.644 | 134.4 |
| O-2 | O-*i* · · · Hw | 1.832 | 2.547 | 129.9 | | | | | |
| O-3 | H(O-*i*) · · · Ow | 1.770 | 2.711 | 172.3 | O-2 | H(O-*j*) · · · Ow | 1.744 | 2.617 | 151.5 |
| O-6 | H(O-*i*) · · · Ow | 1.729 | 2.677 | 178.8 | | | | | |
| O-5′ | O-*i* · · · Hw | 1.838 | 2.634 | 139.6 | O-6′ | H(O-*j*) · · · Ow | 1.727 | 2.653 | 164.4 |
| O-6′ | O-*i* · · · Hw | 1.892 | 2.395 | 110.5 | O-6′ | O-*j* · · · Hw | 1.972 | 2.395 | 104.8 |
| O-2′ | H(O-*i*) · · · Ow | 1.736 | 2.654 | 161.9 | O-3′ | O-*j* · · · Hw | 1.814 | 2.599 | 138.1 |
| O-3′ | H(O-*i*) · · · Ow | 1.740 | 2.658 | 161.8 | O-4′ | H(O-*j*) · · · Ow | 1.826 | 2.576 | 133.8 |
| O-4′ | O-*i* · · · Hw | 1.811 | 2.577 | 135.7 | | | | | |
| O-2′ | O-*i* · · · Hw | 1.780 | 2.516 | 131.9 | | | | | |

[a] Distances in Å; angles in degrees; energies in kcal/mol.

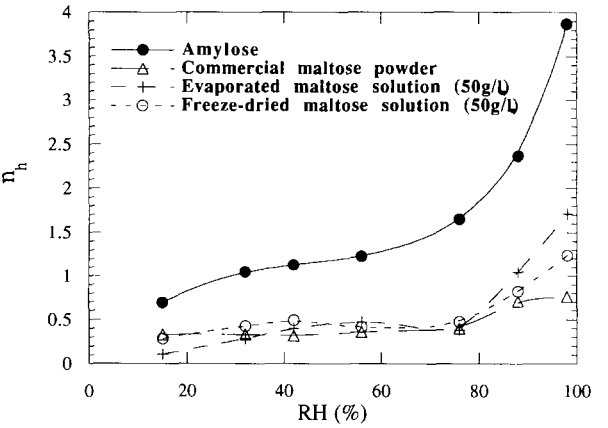


Fig. 4. The number of non-freezing water molecules ($n_h$) as a function of relative humidity (RH) for amylose and $\alpha$-maltose.

amylose, only non-freezing water was observed from 14% to 88% relative humidity.

The DSC curves of crystalline $\alpha$-maltose and of amylose equilibrated at 98% RH exhibit a melting peak at a temperature situated below 0°C. This peak can be attributed to the presence of a small amount of freezing water. Such freezing water was recently put into evidence [1–3,6] when studying hydration of cellulose derivatives and hyaluronic acid. The amount of freezing water decreases when measurements are made using "defatted" amylose (solubilization of Avebe product in dimethyl sulfoxide and precipitation with ethanol). This leads us to attribute the presence of this freezing water to inorganic impurities, as it usually appears in the presence of ionic species.

The quantities of differently adsorbed water were examined by combining the TGA and DSC methods. In Fig. 4, the number of non-freezing water molecules $n_h$ adsorbed per glucose unit is plotted against relative humidity for amylose and differently prepared samples of $\alpha$-maltose. The influence of relative humidity on number of bound water molecules is very different for both compounds. In the case of $\alpha$-maltose, the amount of non-freezing water is almost independent of the relative humidity. It does not seem to depend on the sample preparation method as long as relative humidity does not reach high values (RH < 80%). The quantity of this strongly bound water corresponds approximately to one water molecule per $\alpha$-maltose unit. This number can be linked with the unique water molecule associated with crystal structure of commercial $\alpha$-maltose monohydrate. This comparison clearly indicates that the crystalline areas are unable to fix some other water molecules in the first hydration shell. This statement has been widely used in studies on the hydration of polysaccharides [4,5].

When the relative humidity is high, the non-freezing water content increases and depends on the sample preparation method. This is illustrated by the results given in Table 4 for measurements realised after equilibrium at 98% RH. For freeze-dried samples, the water content increases with dilution of the initial solution. We attribute this to the fact that, in concentrated solution, the interactions between sugar molecules make it easier to crystallise during freeze drying. Consequently, the amorphous part of a

Table 4
Number of non-freezing water molecules ($n_h$) per D-glucopyranose unit in amylose and α-maltose as determined by thermogravimetric analysis and differential scanning calorimetry after equilibrium at 98% RH

| | Amylose | | | Maltose | | |
|---|---|---|---|---|---|---|
| | Commercial | Commercial | Evaporated syrup (50 g/L) | Freeze-dried solution (50 g/L) | Freeze-dried solution (10 g/L) | Freeze-dried solution (1 g/L) |
| $n_h$ | 3.8 | 0.75 | 1.7 | 1.2 | 1.35 | 2 |

sample available for water adsorption and the water quantity is lower than when studying samples based on diluted solution. In the case of samples prepared from evaporated syrup, the water content is higher than the one observed with more diluted solution freeze-dried samples. A rationalisation of this can be based on the different kinetics of drying processes. Whatever the previous considerations are, due to high crystallinity of α-maltose samples, the non-freezing water content is in any case lower than the number of water molecules predicted from the results of molecular modelling. This is understandable, since the packing interactions due to crystal arrangements are not taken into account in molecular modelling and models represent interaction between water molecules and isolated α-maltose molecule.

In the case of α-amylose, the quantity of adsorbed water increases with relative humidity. The curve presented in Fig. 4 is similar to the one obtained when studying some other polysaccharides [2]. In order to rationalise the experimental results, we have analysed the hydration shells obtained from calculations with the different conformers of α-maltose. For this purpose, we have assumed that the hydration pattern of each repeating unit of amylose is similar to that of α-maltose. In this simplified picture, there is one water linked to each of the three hydroxyl groups at 2, 3, and 6 positions of the reductive and non-reductive residue. For M1 and M3 conformers, one water molecule is linked to each of the ring oxygen atoms, whereas for M2 conformer only O-5 is the acceptor of one water molecule. There is no water molecule found to be linked to the glycosidic oxygen atom. Therefore, for a comparison with amylose, we have to discard all water molecules linked to terminal hydroxyl groups at C-4′ and C-1 positions. Each of these hydroxyl groups binds one or two water molecules. One water molecule is bound exclusively by each of these hydroxyl groups, whereas remaining molecules are shared also by other hydroxyl group. Thus, seven or eight water molecules are bound to two repeating units of amylose. Assuming all three α-maltose conformers (six glucopyranose units), 23 water molecules are linked to six glucopyranose residues which gives $n_h = 3.8$ water molecules per D-glucopyranose in amylose. This value is in very good agreement with experimentally observed 3.8 non-freezing water molecules. It is worth comparing these results with a recent investigation on the hydration shell of crystal amylose using Monte Carlo simulations [8]. For a left-handed antiparallel-stranded structure of the amylose double helix, three hydration sites per glucopyranose unit were found. In the case of parallel-stranded double helices, only one hydration site was identified. On the other side, for a solution of glucose and maltose, the hydration numbers of 3.7 and 5.0 were estimated from dielectric and nuclear magnetic relaxation

measurements [29]. Bearing in mind completely different approaches, the agreement between obtained results is striking and strongly suggests the significant role of condensed phase in the hydration of α-maltose and amylose.

## 4. Conclusions

In this work, we have investigated the hydration of α-maltose and amylose using molecular modelling and thermodynamic methods. In agreement with the general trend observed in hydrogen bonding of carbohydrate crystal data, water in complexes with α-maltose displays different hydrogen-bond arrangements. The O · · · H distances involving an acceptor type interaction [i.e. H(O-*i*) · · · Ow] are shorter than those involving donor type interactions [i.e. Hw · · · O-*i*], in agreement with greater acceptor tendency of the water molecule.

The calculated hydration structure of α-maltose appears to be sensitive to the conformation about glycosidic linkage and most of the water molecules are shared by more than one hydroxyl group. Results of differential scanning calorimetry and thermogravimetric measurements suggest that only amorphous phase is available for non-freezing water. The difference in the calculated and observed content of non-freezing water molecules for α-maltose is accounted for by the high crystallinity of α-maltose. This is also supported by good agreement between the observed and estimated number of non-freezing water molecules for amorphous amylose.

## Acknowledgements

One of the authors (C.F.) wishes to thank the CAVISA (Reims, France) for financial support during this study. A grant for supporting the sabbatical stay of one of us (I.T.) was supplied by the Centre National de la Recherche Scientifique (France).

## References

[1] J. Berthold, *Hydration and swelling of wood polymeric constituents*, PhD Thesis, University Joseph Fourier, Grenoble, 1994.
[2] J. Berthold, J. Desbrières, M. Rinaudo, and L. Salmen, *Polymer*, 35 (1994) 5729–5736.
[3] N. Jouon, M. Rinaudo, M. Milas, and J. Desbrières, *Carbohydr. Polym.*, 26 (1995) 69–73.
[4] T.F. Child, *Polymer*, 13 (1972) 259–264.
[5] J.A. Stamm, *Wood Sci. Technol.*, 11 (1977) 39–49.
[6] R.L. Shogren, in C. Ching, D.L. Kaplan, and E.L. Thomas (Eds.), *Biodegradable Polymer Packaging*, Technomic Lancaster, Lancaster, PA, 1993, pp 141–150.
[7] C. Fringant, J. Desbrières, and M. Rinaudo, *Polymer*, submitted for publication.
[8] F. Eisenhaber and W. Schulz, *Biopolymers*, 32 (1992) 1643–1665.
[9] J.W. Brady and R.K. Schmidt, *J. Phys. Chem.*, 97 (1993) 958–966.
[10] M.E. Gress and G.A. Jeffrey, *Acta Crystallogr., Sect. B*, 33 (1977) 2490–2495.
[11] F. Takusagawa and R.A. Jacobson, *Acta Crystallogr., Sect. B*, 34 (1978) 213–218.
[12] S.S. Chu and G.A. Jeffrey, *Acta Crystallogr., Sect. B*, 23 (1967) 1038–1049.

[13] S.N. Ha, L.J. Madsen, and J.W. Brady, *Biopolymers*, 27 (1988) 1927–1952.
[14] V. Tran, A. Buleon, A. Imberty, and S. Perez, *Biopolymers*, 28 (1989) 679–690.
[15] M.K. Dowd, J. Zeng, A.D. French, and P.J. Reilly, *Carbohydr. Res.*, 230 (1992) 223–244.
[16] S. Perez, F.R. Taravel, and C. Vergelati, *Nouv. J. Chim.*, 9 (1985) 561–564.
[17] E.S. Stevens and B.K. Sathyanarayana, *J. Am. Chem. Soc.*, 111 (1989) 4149–4155.
[18] I. Tvaroska, *Biopolymers*, 21 (1982) 1887–1897.
[19] IUPAC-IUB Joint Commission on Biochemical Nomenclature, *Eur. J. Biochem.*, 131 (1983) 5–7.
[20] N.L. Allinger, Y.H. Yuh, and J.-H. Lii, *J. Am. Chem. Soc.*, 111 (1989) 8551–8566.
[21] N.L. Allinger, M. Rahman, and J.-H. Lii, *J. Am. Chem. Soc.*, 112 (1990) 8293–8307.
[22] P. Huyskens and D. Peeters, *J. Mol. Struct.*, 300 (1993) 539–550.
[23] D. Peeters and G. Leroy, *J. Mol. Struct.*, 314 (1994) 39–47.
[24] G.A. Jeffrey, *Acta Crystallogr., Sect. B*, 46 (1990) 89–103.
[25] G.A. Jeffrey and H. Maluszynska, *Acta Crystallogr., Sect. B*, 46 (1990) 546–549.
[26] G.A. Jeffrey, *J. Mol. Struct.*, 322 (1994) 21–25.
[27] P. Gilli, V. Bertolasi, V. Ferretti, and G. Gilli, *J. Am. Chem. Soc.*, 116 (1994) 909–915.
[28] H. Yoshida, T. Hatakeyama, and H. Hatakeyama, in W.G. Glasser and H. Hatakeyama (Eds.), *Viscoelasticity of Biomaterials*, ACS Symp. Ser. 489, American Chemical Society, Washington, DC, 1992, pp 217–230.
[29] A. Suggett, *J. Solution Chem.*, 5 (1976) 33–46.